Pergamon

Journal of Structural Geology, Vol. 19, No. 9, pp. 1189 to 1200, 1997

0191-8141/97 $17.00 + 0.00

PII: S0191-8141(97)00043-6

Finite strains in transpression zones with no boundary slip

BEN J. DUTTON

Department of Earth Sciences, Parks Road, Oxford OX1 3PR, U.K.

(*Received* 12 *February* 1996; *accepted in revised form* 12 *May* 1997)

Abstract—A mathematical model describing finite strains has been developed for transpression zones where no slip is allowed in any direction at the zone boundaries. This has been adapted to model transpression zones where the boundaries are inclined. The model can also be used to describe finite-strain patterns where material is incorporated into the deforming zone from one or both sides after the initiation of deformation, so that the deforming zone remains at a constant width, thus allowing large transpressional strains to be accommodated without the deforming zone closing to zero thickness. This model of 'steady-state' transpression can be used to explain some of the features of the South Mayo Trough, a late Silurian transpression zone in the west of Ireland. © 1997 Elsevier Science Ltd.

INTRODUCTION

Transpression is the deformation caused by two obliquely converging zones, as defined by Harland (1971). Sanderson and Marchini (1984) were the first to describe such a deformation in terms of its kinematics. They considered a zone with neither volume loss nor horizontal slip at the boundaries, so that the shortening across the zone results in vertical extrusion (Fig. 1a). They factorized the deformation into simple-shear and pure-shear strain components and used the resulting matrix to model its kinematics.

The Sanderson and Marchini (1984) model has been expanded by Fossen and Tikoff (1993) who also allowed for volume loss. Dias and Ribeiro (1994) used a similar method to model lateral escape (as opposed to vertical escape), vertical shear, compaction and tectonic volume loss. Tikoff and Teyssier (1994), Jones and Tanner (1995) and Teyssier *et al.* (1995) considered the effects of strain partitioning in transpression zones, where part or all of the strike-slip component of strain partitions into discrete, zone-boundary-parallel fault zones.

One important limitation of the Sanderson and Marchini (1984) model was pointed out by Schwerdtner (1989); the zone boundaries are frictionless vertically, to allow the deforming zone to extrude, yet to transmit the simple-shear strain they must allow no slip horizontally—an unlikely scenario in real transpression zones. Robin and Cruden (1994) overcame this problem by allowing no slip in any direction at the zone boundaries, resulting in a heterogeneous deformation across the zone, causing the material to bulge out at the centre (Fig. 1b). Robin and Cruden (1994) considered only instantaneous strain. By using an approach initially similar to that of Robin and Cruden (1994), the first aim of this paper is to extend their work, and investigate the variations of finite strain across a transpression zone where no slip is allowed at the zone boundaries.

Another problem common to all transpression models is that they can only accommodate a finite amount of shortening across the deforming zone before the zone boundaries meet, so that no further transpressive strain can be accommodated. The second aim of this paper is to develop a model of 'steady-state' transpression, where

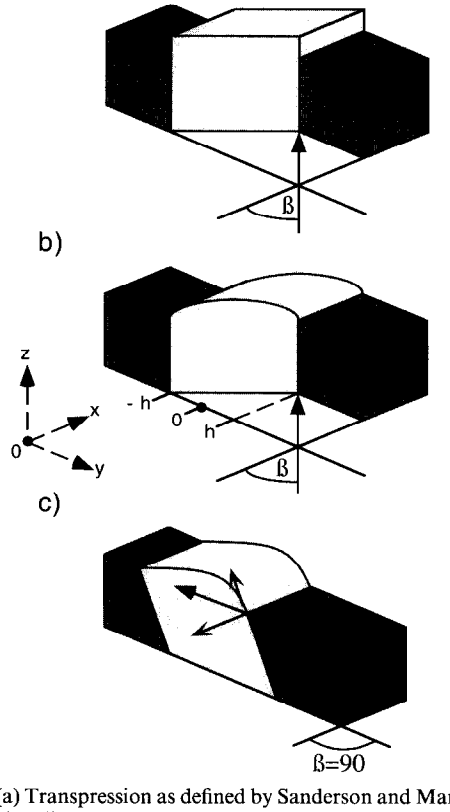

Fig. 1. (a) Transpression as defined by Sanderson and Marchini (1984). Boundaries allow no slip horizontally, yet are frictionless vertically. β is the angle between the zone boundary in the horizontal plane and the movement direction. (b) Transpression as defined by Robin and Cruden (1994) with no slip in any direction allowed on the zone boundaries. β is the angle between the movement direction and the zone boundary, as first defined by Sanderson and Marchini (1984). Also defined is the coordinate system used. The z-direction is vertical, y is perpendicular to the zone boundaries, and x is horizontal and parallel to the zone boundaries, with the origin being shown by the black dot. The velocities u, v and w act in the x-, y- and z-directions, respectively. (c) Inclined transpression, for a value of β of 90°. δ is the dip of the zone boundaries, as well as the angle between the zone boundary in the vertical plane and the movement direction.

the deforming zone maintains a constant width, so that infinite strains can be accommodated.

MODEL

The deforming zone is modelled as being rheologically homogeneous. The zone boundaries allow for no slip in any direction, so the vertical extrusion of material from the zone becomes concentrated towards its centre, setting up a vertical shear gradient across the zone. The pure-shear strain component is therefore heterogeneous. The model initially follows the method used by Robin and Cruden (1994). Equations for the velocities of particles caused by the pure-shear deformation described above are given as functions of the zone width and coordinate positions in the zone by Jaeger (1962, p 140). Changing some of Jaeger's coordinates to fit with the coordinates used in this paper (see Fig. 1b), namely Jaeger's x coordinate for z and Jaeger's u velocity for w, results in equations (1a) and (2).

The simple-shear strain is distributed evenly across the entire deforming zone, so the velocity at any given point in the zone can be found (Fig. 2). As an angular relationship between the pure-shear and simple-shear strains is required, the velocity of the zone boundaries in the x-direction (U) is given in terms of the velocity of the zone boundaries in the y-direction (V), and the angle between U and the total displacement vector. Following Sanderson and Marchini (1984) this angle has been named β. The velocity in the x-direction can therefore be given in equation (3)

If the zone boundaries are not vertical, but inclined, and the zone-boundary movement remains horizontal, then a relative vertical shear occurs (Fig. 1c). Robin and Cruden (1994) named this vertical shear 'oblique transpression'. As the term 'oblique convergence' is already used for transpression generally, the term 'inclined transpression' is used for the vertical shear strain produced by the approach of inclined boundaries. The amount of vertical shear is described by δ, the dip of the zone boundaries, which coincides with the angle between the zone boundaries and the movement direction when $\beta = 90°$ (see Fig. 1c). To calculate the strain caused by inclined boundaries the model is run with vertical zone boundaries and appropriate vertical shear calculated from δ, and the zone is then re-orientated to the correct dip for the zone boundaries. The velocity in the z-direction, w, caused by inclined transpression can be found by exactly the same method as for the velocity in the x-direction caused by the horizontal simple shear, and is given in equation (1b)

$$w = \frac{3Vz(h^2 - y^2)}{2h^3} \tag{1a}$$

$$w' = Vy/h \tan(\delta) \tag{1b}$$

$$v = \frac{3Vy(y^2 - 3h^2)}{2h^3} \tag{2}$$

$$u = Vy/h \tan(\beta), \tag{3}$$

where x, y and z are position coordinates (as in Fig. 1b); u, v and w are velocities in the x-, y- and z-directions, respectively; V is the velocity of approach of two boundaries; U is the total velocity across the zone, parallel to the zone boundaries; h is the zone half-width; β is the angle between the zone boundary and displacement direction in the horizontal plane; and δ is the angle between the zone boundary and displacement direction in the vertical plane, or the dip of zone boundaries.

Following the method of Robin and Cruden (1994), equations (1a), (1b), (2) and (3) are differentiated to form the velocity gradient tensor, **L**. Note that this is different from the velocity gradient tensor given in Robin and Cruden (1994). This is partly to do with the different definitions of β, partly due to Robin and Cruden's use of strain rate parameters and normalized heights and widths, and partly due to a typing error in their dw/dz term

$$\mathbf{L} = \begin{pmatrix} 0 & \dfrac{V}{h\tan(\beta)} & 0 \\ 0 & -\dfrac{3V(h^2 - y^2)}{2h^3} & 0 \\ 0 & \dfrac{V}{h\tan(\delta)} - \dfrac{3Vyz}{h^3} & \dfrac{3V(h^2 - y^2)}{2h^3} \end{pmatrix}. \tag{4}$$

As the velocity gradient tensor is independent of x, it describes a section perpendicular to the zone boundaries across an infinitely long deforming zone with no variation in the x-direction.

The incremental deformation gradient tensor, $\mathbf{F}_I$, can be found by multiplying **L** by dt, and adding the unit matrix, **I**

$$\mathbf{F}_I = \mathbf{L}\, dt + \mathbf{I}. \tag{5}$$

By calculating a series of incremental deformation gradient tensors and sequentially pre-multiplying each,

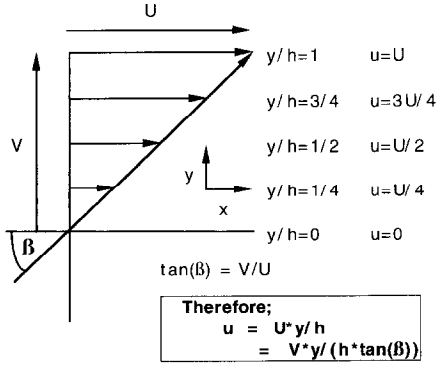

Fig. 2. The formation of equations describing the velocity variation across the deforming zone caused by the simple-shear component of strain. See text for parameter definitions.

the finite deformation gradient tensor **F** can be approximated

$$\mathbf{F} = \mathbf{F}_1\mathbf{F}. \quad (6)$$

As the deforming zone narrows, particles move relative to each other and to the approaching zone boundaries. As **L** is a function of y, z and h, these parameters need to be updated after each increment using equations (1a) and (2) to find the positions of each point and the new zone half-width. These are then used for calculating the next incremental deformation gradient tensor to be pre-multiplied. This iteration is repeated until the required strain, measured by the shortening of the zone-boundary half-width, has been reached.

The final step is to calculate the values and orientations of the principal axis of the finite-strain ellipsoid. **F** is decomposed into a stretch component, **U**, and a rotation component, **R** (see Malvern, 1969, chap. 4) such that

$$\mathbf{F} = \mathbf{UR}, \quad (7)$$

where

$$\mathbf{U} = (\mathbf{F}^{\mathrm{T}}\mathbf{F})^{1/2} \quad (8)$$

and

$$\mathbf{R} = \mathbf{U}^{-1}\mathbf{F}. \quad (9)$$

The lengths of the principal axis of the finite-strain ellipsoid can then be calculated by finding the eigenvectors of **U**, and the orientations of the finite-strain ellipsoid found by pre-multiplying the eigenvectors of **U** by **R**.

To describe the symmetry of the strain, Flinn's k value is found, using

$$k = \frac{s_1/s_2 - 1}{s_2/s_3 - 1} \quad (10)$$

and the strain intensity, d, is calculated using

$$d = \sqrt{(s_1/s_2 - 1)^2 + (s_2/s_3 - 1)^2}, \quad (11)$$

where s_1, s_2 and s_3 are the lengths of the long, intermediate and short axes, respectively, of the finite-strain ellipsoid. The strain intensity, d, represents the strain on a Flinn plot, measured as the distance from the (1, 1) origin, and is therefore dimensionless.

Jaeger's equations (Jaeger, 1962) describe the flow of material moving out of the zone vertically in two opposite directions between the two approaching plates. The model presented in this paper therefore predicts the flow upwards and downwards out of the deforming zone, with positive z coordinates resulting in upward extrusion, and negative z coordinates resulting in downward extrusion. However, for Jaeger's equations to be valid, the flow out of the deforming zone must be uninhibited. Whereas this may be the case for the upward extrusion, with the top of the model representing the surface of the Earth, it is not the case for the downward movement, which is impeded by the lower crust and/or the mantle. However, it is likely that in a transpression zone there will be a roughly horizontal plane above which material will flow freely upward and below which material will flow downward. Jaeger's equations should still be valid for regions above this plane, where z is positive. To avoid problems close to this plane, only results with a height equal to or above the width of the deforming zone are considered.

Implementation

Matlab® matrix operations program, running on a UNIX work station, was used to write programs to perform the above calculations and plot results for a spread of points across the zone. The method used to calculate the finite strain is an approximation, with the results becoming more accurate the smaller the value of dt used. A value of 0.001 was used for dt; reducing this value resulted in negligible differences in the results, but extended the running time of the program from hours into days. To check on the accuracy of the model the volume loss was calculated for each point. All values calculated were less than 1%, which compare well with the theoretical value of zero. In addition, the model was run for pure wrenching, with the results exactly matching those predicted by theory (Ramsay, 1967). The model was also run for one iteration, and produced similar results to the instantaneous strain calculated by Robin and Cruden (1994).

RESULTS

The predicted particle displacement paths described by an array of points with uniform final positions are shown in Fig. 3. Note that it is the values of y and z relative to each other and to the zone half-width, h, that are important rather than their absolute values. The axes of the plot in Fig. 3 and subsequent plots are therefore labelled in terms of multiples of the final zone half-width, h. This has the implication that the model can be scaled by any factor, to compare with real transpression zones of any size.

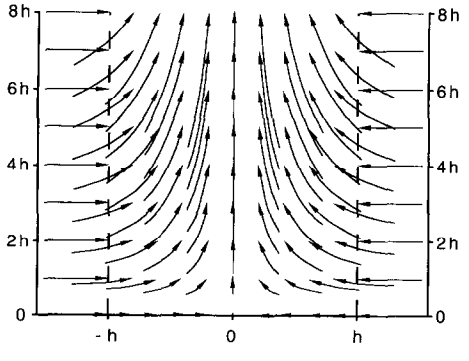

Fig. 3. Particle displacement paths for $\alpha = 67\%$ in terms of the final half-width, h. Dashed lines indicate final zone-boundary positions. Displacement paths are chosen to give a uniform final distribution.

The ratio of final to initial zone half-widths, expressed as a percentage and called α, is used to measure the deformation applied to the transpression zone. Results predicted by the model for different α, β and δ values are shown in Figs 4–12. In these figures, and in the subsequent descriptions, the term 'foliation' is used to describe the plane containing the long and medium axis of the finite-strain ellipsoid, and the term 'lineation' is used to describe the long axis of the finite-strain ellipsoid (cf. Robin and Cruden, 1994).

Strain intensity

The simple-shear strain intensity is constant across the deforming zone, but the pure-shear strain intensity varies with position in the zone. Figure 4 shows this variation in pure-shear strain intensity for different α values. For $\alpha = 66\%$, the strain intensity is higher at the edges of the zone than in the centre at any one height. For $\alpha = 33\%$, at any one height the strain is at a minimum somewhere between the edge and the centre of the zone, with the maximum strain intensity being either on the zone boundary or in the centre of the zone depending on height. For all α values, strain intensity increases with increasing height.

Foliation patterns

The patterns of foliation for $\alpha = 66\%$ (Figs 5 & 6) are similar to those predicted by Robin and Cruden (1994) for instantaneous strain. The foliations are, in general, vertical and more oblique to the zone boundaries in the centre of the zone, and less steep but more parallel to the zone boundaries at the edge of the zone. The patterns for finite strain are everywhere steeper and more parallel to the zone boundaries than for instantaneous strain. With lower β values, the foliations are increasingly oblique to the zone boundaries. As noted by Robin and Cruden (1994), the variation in foliation strike is opposite to that predicted within shear zones by Ramsay and Graham (1970). In Ramsay and Graham (1970) type shear zones foliation will initially be oblique (45°) to the zone boundaries. It is the concentration of the simple-shear strain in the centre of the zone which causes fabric rotation to be greatest in this region, resulting in the foliation having a maximum obliquity to the shear-zone boundaries at the edges of the zone. In the transpression model presented here, the pure-shear strain is greatest at the edges of the zone, so the foliation tends to be more parallel to the zone boundaries in this region, whereas in the centre of the zone the simple-shear strain is relatively larger, so the foliation is more oblique to the zone boundaries. As the simple-shear strain is evenly distributed in the transpression model, there is no increased rotation of fabrics in the centre of the zone as in the Ramsay and Graham (1970) type shear zone.

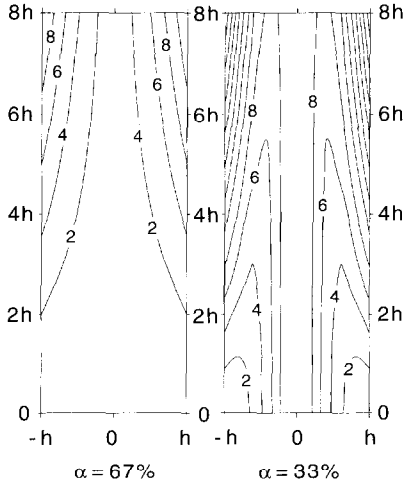

Fig. 4. Strain intensity variations for the pure-shear strain component of transpression for deformation zone shortening of $\alpha = 67\%$ (left) and $\alpha = 33\%$ (right). Contours are in intervals of two dimensionless units. See text for calculation and discussion.

For increased shortening across the zone, to $\alpha = 33\%$ (Fig. 7), the foliation patterns have a double swing in strike, from parallel to the zone boundary at the edge of the zone, becoming more oblique initially moving towards the centre of the zone, but then becoming less oblique to the zone boundaries in the centre. This is due to the relative importance of the pure-shear to simple-shear components. For larger amounts of shortening across the deforming zone, the pure-shear strain intensity is complex (see Fig. 4). The strains are highest at the zone boundaries and in the centre of the zone, with two minima either side of the centre of the zone. Where the pure-shear strain is high, the foliation is more parallel to the zone boundaries, where it is lower the foliation is more oblique, resulting in the double swing in strike.

Lineation patterns

Lineations in this model of transpression are almost always sub-vertical except in the centre of zones where $\alpha > 55\%$, and β is less than 13.28°. In this case the lineation is horizontal. However, as mentioned by Robin and Cruden (1994), when the lineation is horizontal the k value is less than 0.3, so that the lineation would not be expected to be seen in the field. The β value of 13.28° corresponds to Robin and Cruden's 'press'/'trans' ratio of 0.234. This β value is lower than predicted by the Sanderson and Marchini (1984) model, where the switch from a vertical to horizontal stretching lineation occurs at $\beta = 19.5°$, which is due, as Robin and Cruden (1994) pointed out, to the concentration of the extrusion in the centre of the zone. This also explains why the switch from a horizontal to a vertical stretching lineation occurs at lower strains in this model than in the Sanderson and Marchini model for a set β value (compare Fig. 8 with fig. 7, 10° path of Sanderson and Marchini, 1984).

The azimuth of the lineation has a large variation depending on β. For $\beta = 10°$, the lineation is sub-parallel to the strike of the zone boundaries (Fig. 6), whereas for

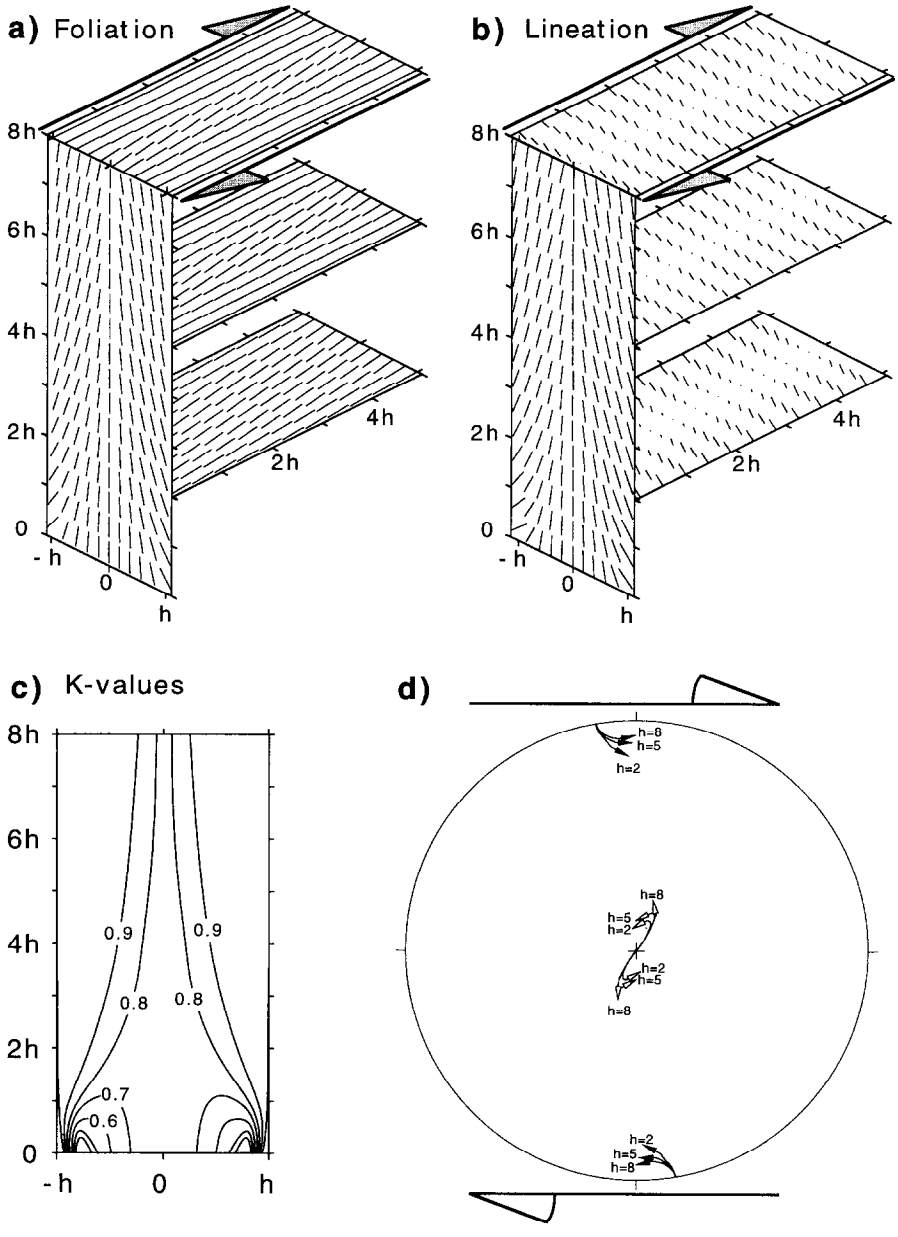

Fig. 5. Deformation patterns for $\beta = 50°$, $\delta = 90°$ and $\alpha = 67\%$. (a) Foliation and (b) lineation patterns. Horizontal layers are at heights of $2h$, $5h$ and $8h$ after deformation. (c) k value patterns. (d) Lower-hemisphere, equal-area stereoplot of poles to foliation (solid arrow heads) and lineation (hollow arrow heads). Arrows point from the centre of the zone to the edge.

lower β values the lineation is sub-perpendicular to the strike of the zone boundaries (Fig. 5). With increased shortening across the deforming zone, the lineation becomes rotated towards parallelism with the zone boundaries (Fig. 7). As with the foliation, although less marked, there is a swing in the azimuth of the lineation from the edge to the centre of the zone.

k *value patterns*

At the edge of the deforming zone the k value is always equal to 1, and generally decreases towards the centre of the zone, with the minimum value dependent on the β value and the α value. There is a complex pattern of k values at the base of the zone for β values greater than 13.28°. The complex area at the base of the zone is larger with decreasing α values, so that for levels less than $4h$ high k values may at first decrease towards the centre of the zone but then increase again.

The Flinn plot in Fig. 8 shows how the k value varies, with decreasing α values, for a β value of 10° at a level of $4h$. The 'bouncing' of the $y = 0$ path off the $k = 0$ axes of Fig. 8 coincides with the change in plunge of lineation from horizontal to vertical.

INCLINED TRANSPRESSION

Robin and Cruden (1994) pointed out that in many real transpression zones the strain is asymmetric,

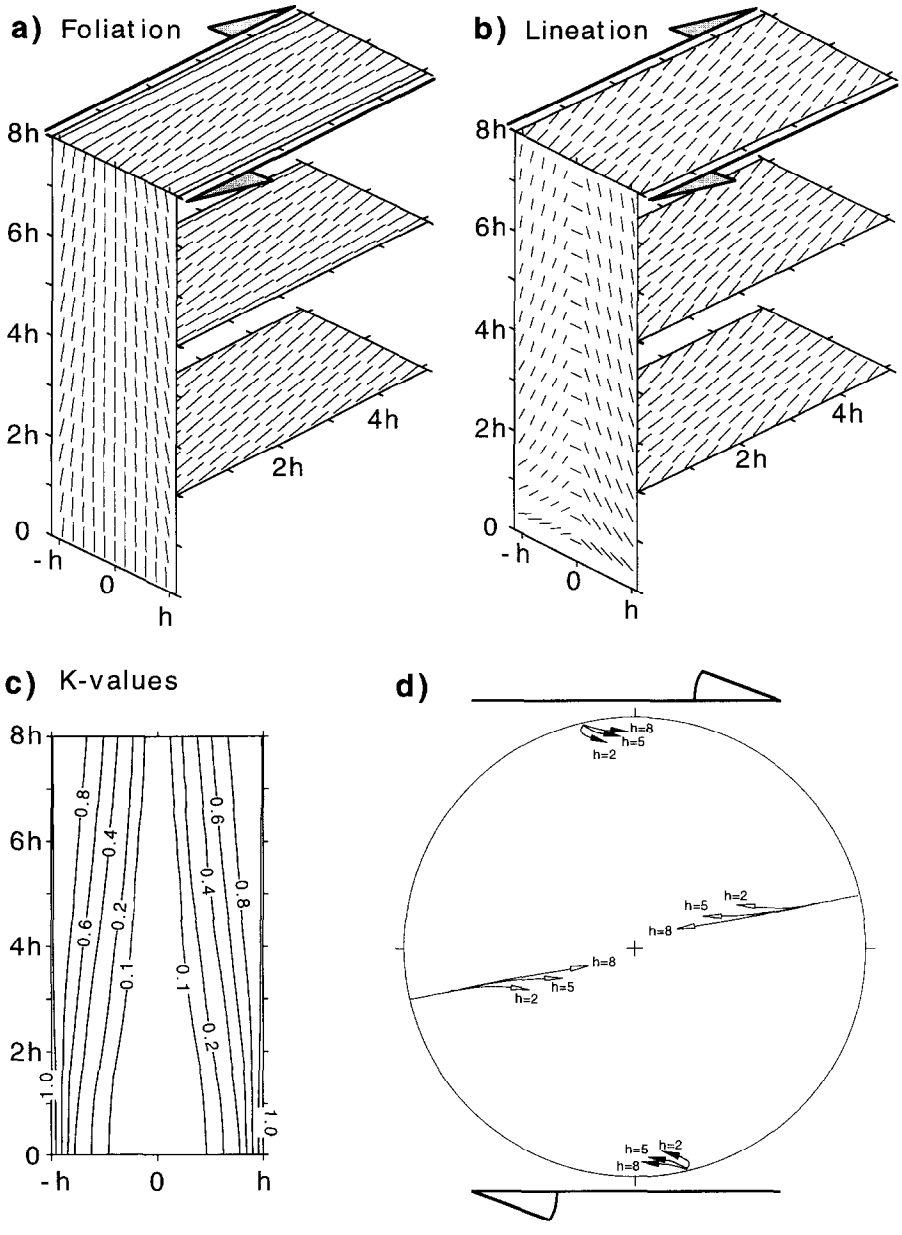

Fig. 6. Deformation patterns for $\beta = 10°$, $\delta = 90°$ and $\alpha = 67\%$. (a) Foliation and (b) lineation patterns. Horizontal layers are at heights of $2h$, $5h$ and $8h$ after deformation. (c) k value patterns. (d) Lower-hemisphere, equal-area stereoplot of poles to foliation (solid arrow heads) and lineation (hollow arrow heads). Arrows point from the centre of the zone to the edge. Note that most of the variation in the plunge of the lineation is in a narrow zone in the centre of the deforming zone.

whereas the model above predicts only symmetrical transpression zones. Robin and Cruden (1994) created asymmetrical transpression by moving one of the zone boundaries vertically with respect to the other, again for instantaneous strain only. Purely vertical movements in the Earth's crust are not commonly observed, but if the boundaries of the deforming zone are inclined to the vertical (whilst still remaining parallel), and the transport direction remains horizontal, then the boundary walls will move relative to each other to create a shear component parallel to the dip of the zone boundaries (Fig. 1c). This has been modelled by introducing a vertical shear component to the model, then tilting the model by the required angle. The results are plotted in Fig. 9, with the amount of vertical shear being indicated by δ, the dip of the zone boundaries.

Features predicted by the model with vertical zone boundaries are still present, but there is now an asymmetry to the deformation. This asymmetry is small, particularly for foliation and lineation orientations, until the zone boundaries are almost flat-lying, with dips of 10°. Whereas these dips may be reasonable for oblique thrust–ramp systems, they are not for the majority of transpression zones which tend to be steep (Sanderson and Marchini, 1984). It is therefore believed that inclined transpression cannot be responsible for making strongly asymmetrical transpression zones.

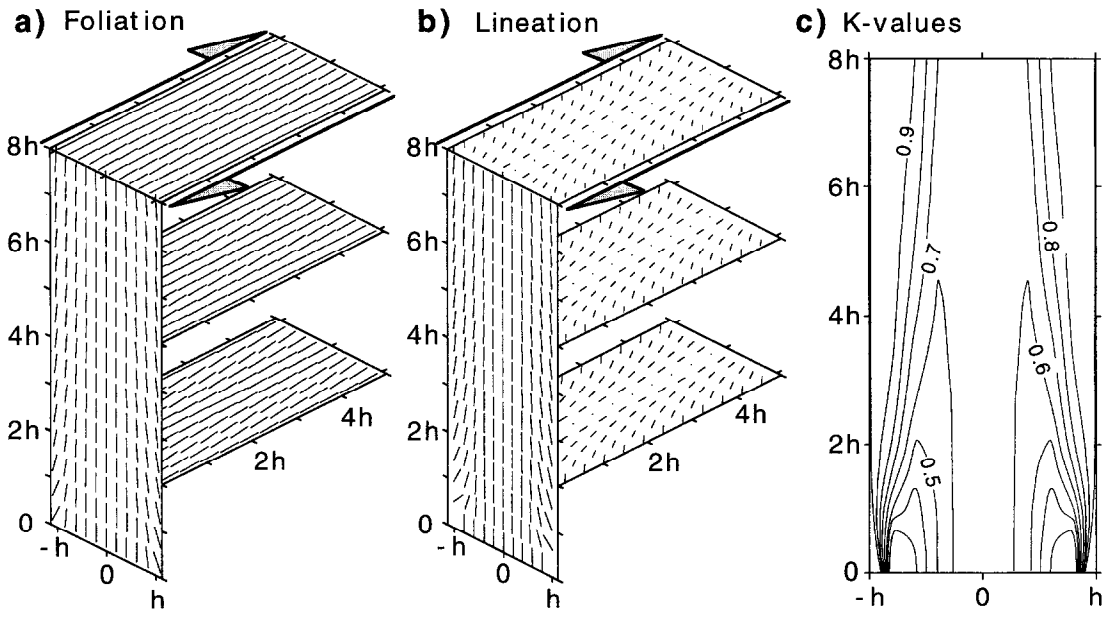

Fig. 7. Deformation patterns for $\beta = 50°$, $\delta = 90°$ and $\alpha = 33\%$. (a) Foliation and (b) lineation patterns. Horizontal layers are at heights of $2h$, $5h$ and $8h$. (c) k value patterns.

STEADY-STATE TRANSPRESSION

A problem common to all models of transpression to date (e.g. Sanderson and Marchini, 1984; Dias and Ribeiro, 1994; Robin and Cruden, 1994; Tikoff and Teyssier, 1994) is that they can only accommodate a finite amount of displacement across the deforming zone before the zone boundaries meet and all of the deforming zone has been extruded to infinite strains. This problem can be tackled in one of two ways. Either (1) the pure-shear strain component diminishes over time, with the transpression becoming more and more wrench dominant until the deforming zone is a narrow strike-slip deformation zone (Fig. 10a) or (2) new material is constantly added to the deforming zone from the zone boundaries at a rate equal to (or greater than) the vertical expulsion of rock from it, thus resulting in a constant (or growing) deformation zone thickness (Fig. 10b).

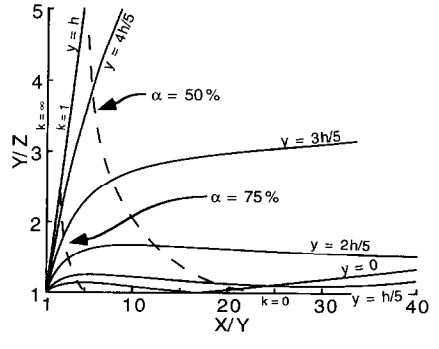

Fig. 8. Flinn plot for increasing strain for various points across the deforming zone at height $z = 4h$ and $\beta = 10°$. The dashed lines represent the strain when the zone has been shortened to 75% and 50% of its original width.

This steady-state transpression has been modelled by keeping the zone-boundary half-width (h) constant, but otherwise running the model in the same way as previously. Points are periodically added at the edge of the zone to record the strain of new material incorporated in to the zone. The results of this modelling for $\beta = 10°$ and $\delta = 90°$ are shown in Fig. 11.

The strain intensity for the pure-shear strain component for steady-state transpression can be seen in Fig. 11(c). There are two maxima at the top of the deforming zone, at $h = \pm 0.5$, with strain intensity being lowest at the edges of the deforming zone. The k values for steady-state transpression have similar patterns for non-steady-state transpression (Fig. 11b). The foliations for steady-state transpression have maximum obliquity and minimum dips at the zone boundaries, with variations in orientation being dependent on the height in the zone. Lineations have the lowest plunge and an azimuth nearly perpendicular to the zone boundaries at the edges of the zone (except for the special case where $\beta < 13.28°$ for $\alpha > 55\%$, where lineation is horizontal in the centre of the zone). Towards the centre of the deforming zone, lineations generally become steeper and more parallel to the zone boundaries.

The variations in strain described above are all due to the fact that regions close to the zone boundaries have been introduced to the deforming zone later than points further in towards the centre, and have therefore undergone less deformation.

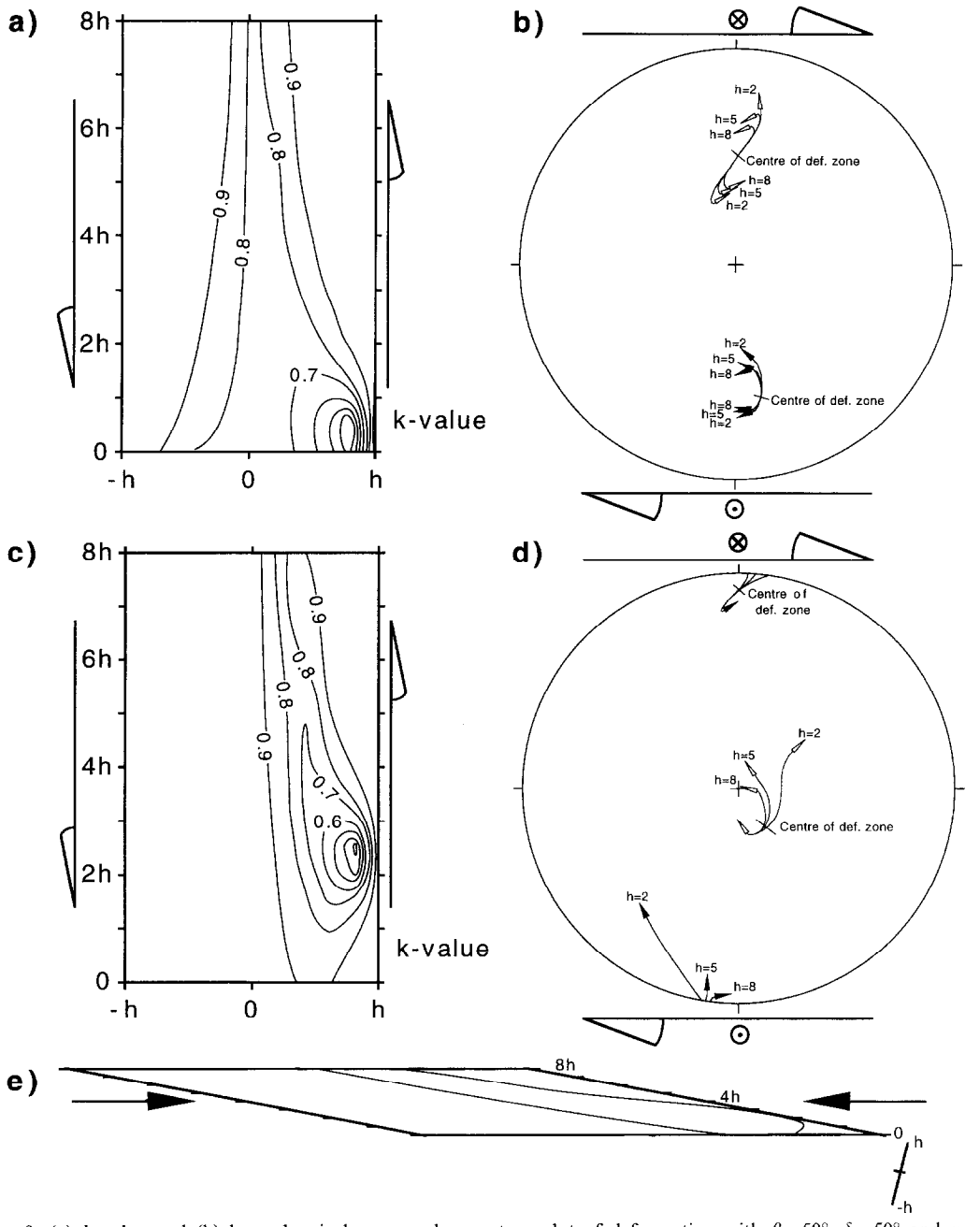

Fig. 9. (a) k value and (b) lower-hemisphere, equal-area stereoplot of deformation with $\beta = 50°$, $\delta = 50°$ and $\alpha = 67\%$. Foliation is represented by solid arrow heads and lineation by hollow arrow heads. Arrows point from the centre of the zone to the edge. (c) k value and (d) lower-hemisphere, equal-area stereoplot of deformation with $\beta = 50°$, $\delta = 10°$ and $\alpha = 67\%$. The k values have been plotted in (a) and (c) so that they are easy to read. The actual shape and orientation of the deformed zone for a zone-boundary dip of 10° is shown in (e). The height labels on the stereoplots relate to horizontal levels after tilting, not to the height levels in the original models.

ASYMMETRIC STEADY-STATE TRANSPRESSION

If the new material added to the deforming zone comes from one side only, as in Fig. 10(c), asymmetric fabric patterns are developed (Fig. 12). The pure-shear strain intensity varies asymmetrically across the deforming zone (Fig. 12c), while the k value patterns become a skewed version of that for symmetric steady-state transpression, with lower k values nearer the fixed zone boundary. The azimuth of the lineation varies from sub-parallel to the zone boundary at the fixed boundary to sub-perpendicular at the opposite boundary. The plunge of the lineation remains sub-vertical throughout most of the deforming zone, but on the non-fixed boundary the plunge decreases to 45°. The foliation patterns show a similar asymmetry, striking sub-parallel to the zone boundary with a sub-vertical dip at the fixed edge, and striking and dipping at 45° to the zone boundary on the opposite edge. At lower levels the pattern becomes

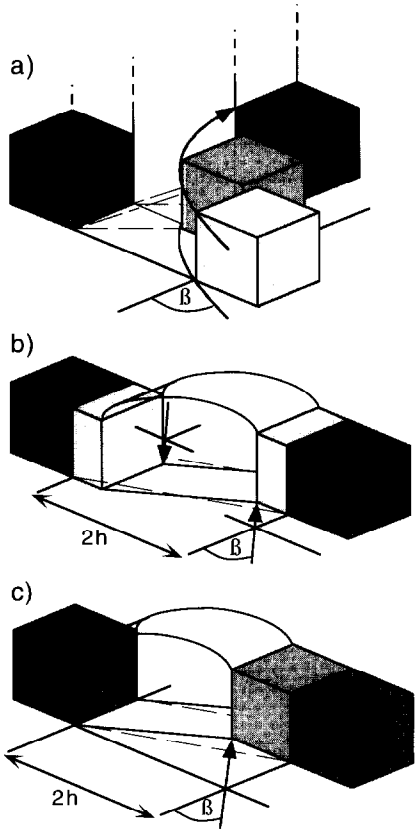

Fig. 10. (a) Steady-state transpression accommodated by the β value progressively reducing to 0°, so the deforming zone does not disappear completely. The zone therefore becomes one of horizontal simple-shear, not transpression. (b) Symmetrical steady-state transpression where the deforming zone 'grows' at both sides and (c) asymmetrical steady-state transpression where the deforming zone 'grows' on one side only, with the increasing approach of the zone boundaries. Dashed lines indicate the new position of the boundaries. Note that in the model this growth occurs incrementally, not in one step as indicated here.

slightly more complex, due to the complex pure-shear strain component.

THE SOUTH MAYO TROUGH

The asymmetric steady-state transpression model could create the asymmetrical strain observed in many transpression zones. This may be caused by a strong rheological contrast across one boundary of the deforming zone, as is the case in the transpression zone which deformed the South Mayo Trough, western Ireland.

The South Mayo Trough consists of low-grade Ordovician and Silurian sediments, forming a 20 km wide, E–W-trending synclinorium. The fold-axial surface of this, and other smaller folds in the area, is always steeply dipping, with an E–W-trending sub-vertical fold axis. The Ordovician sediments were deposited in a forearc basin, conformably on top of an ophiolite basement, during limited N–S syn-depositional shortening (Dewey and Ryan, 1990). The Silurian sediments were deposited in three geographically and temporally separate basins unconformably on top of the Ordovician sediments, and the whole area subsequently deformed in the late Silurian–early Devonian under sinistral transpression by the relative movements of the Dalradian blocks of North Mayo and Connemara (Hutton and Dewey, 1988). The strain associated with the transpressive event is very weak in the south, and increases northwards to a maximum against the Silurian–Dalradian boundary (McKerrow and Campbell, 1960; Dewey, 1967). This northern boundary to the transpressive event not only divides deformation styles, but also forms a

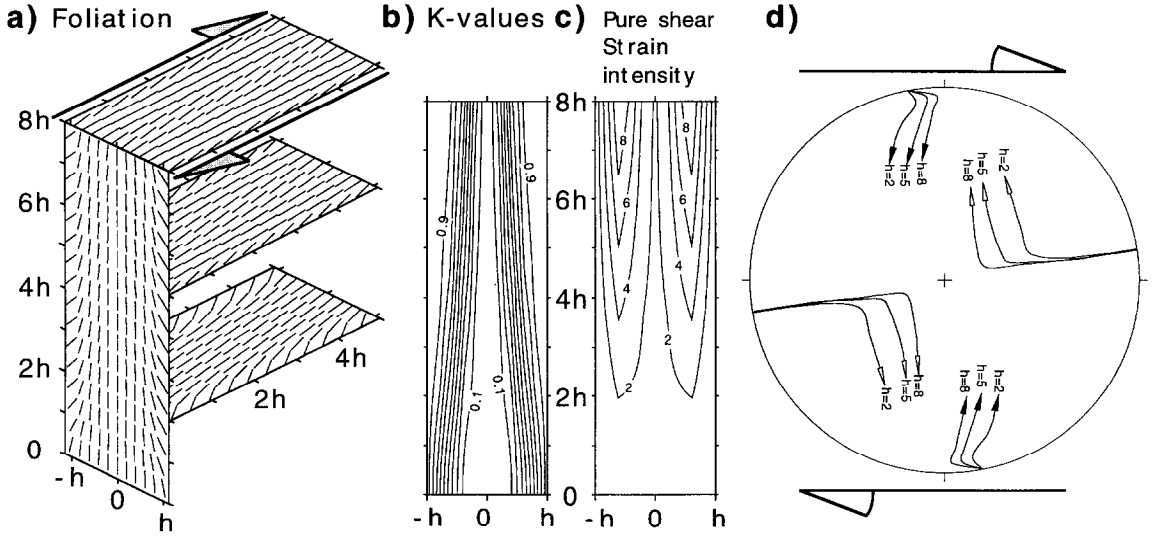

Fig. 11. Deformation patterns for steady-state transpression, $\beta = 10°$, $\delta = 90°$ and $\alpha = 50\%$. (a) Foliation, (b) k value, (c) pure-shear strain component strain intensity in dimensionless units and (d) lower-hemisphere, equal-area stereoplot of foliation (solid arrow heads) and lineation (hollow arrow heads). Arrows point from the centre of the zone to the edge. The strain applied is equivalent to $\alpha = 50\%$, the original deforming zone has halved in width.

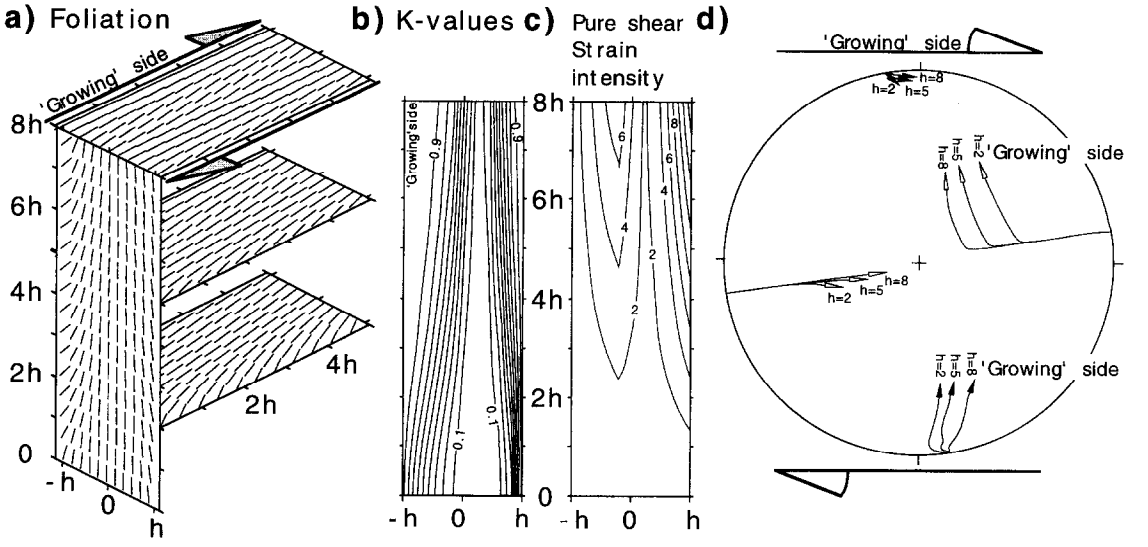

Fig. 12. Deformation patterns for asymmetric steady-state transpression, $\beta = 10°$, $\delta = 90°$ and $\alpha = 50\%$. (a) Foliation, (b) k value, (c) pure-shear strain component strain intensity in dimensionless units and (d) lower-hemisphere, equal-area stereoplot of foliation (solid arrow heads) and lineation (hollow arrow heads). Arrows point from the centre of the zone to the edge. The strain applied is equivalent to $\alpha = 50\%$ (the original deforming zone has halved in width). The side of the zone through which new material is incorporated into the deforming zone is indicated as the 'growing' side.

rheological boundary between relatively weak sediments to the south and the relatively strong, metamorphosed rocks of the Dalradian block to the north. The southern boundary to the transpressive deformation is not well defined, as the strain dies out gradually southwards. It is, therefore, tentatively proposed that the deformation could have formed in a way similar to the asymmetric steady-state transpression model. The deformation initially was concentrated at the northern boundary of the trough. After a certain point in time this initial zone could no longer accommodate the strain applied, so the deforming zone widened. To the north of the zone lies the relatively hard, metamorphosed Dalradian block, so the zone widened southwards only thus creating an asymmetrical strain pattern in the rocks.

The northern part of the South Mayo Trough has been mapped by the author to determine the orientation of foliation and lineation, and the strain variation across the area. Data taken from a N–S section across South Mayo are shown in Fig. 13. To the west of this section later folding effects the rocks (Kelly and Max, 1979), but foliation and lineation have the same orientation as shown in Fig. 13 once the rotation caused by the folding has been removed. These field data are compared to the asymmetric steady-state transpression model ($\beta = 50°$, $\delta = 45°$), corresponding to the dip of the northern zone boundary of the South Mayo Trough (Ryan *et al.*, 1983) with a contraction of 50%, approximately the shortening indicated by the folding in the northern region of the trough (Dewey, 1967). The orientation of foliation and lineation predicted by the model are shown in Fig. 13(d).

There is a single conglomerate bed of variable thickness which crops out on the southern and northern margin of the Croagh Patrick Silurian. The k values of the strain in this conglomerate, determined using the R_f/ϕ method (Lisle, 1985) from field photographs of the principle planes of strain, are all less than 1 but vary greatly from outcrop to outcrop making a comparison with the model impossible. This variation also means an accurate comparison of strain intensity between the model and the South Mayo Trough is not possible. The model predicts that, overall, the strain at the fixed boundary has a higher intensity than at the 'growing' boundary. This compares favourably with field observation, where the strain is at its maximum in the north (the fixed boundary) and falling away to zero at the southern margin of the trough (Ryan and Dewey, 1991).

The model predicts foliation to have an approximately constant WNW–ESE strike, with a sub-vertical dip in the south changing to a steep northerly dip in the north. The foliation in the South Mayo Trough has these orientations. Whereas the model predicts that the lineation should be steep, with a complex azimuth variation, the stretching lineation in the South Mayo Trough is weak with a sub-horizontal plunge, E–W in the south and NE–SW in the north. This difference may be due to the folding in the rocks of the South Mayo Trough which accommodates vertical extension but not the required horizontal component. The latter has resulted in fold-axis parallel stretching forming a sub-horizontal stretching lineation. This strain partitioning between the folding and the stretching lineation is not part of the transpression model, which predicts the orientation of overall maximum extension, thus providing a possible explanation for the difference between it and the field data.

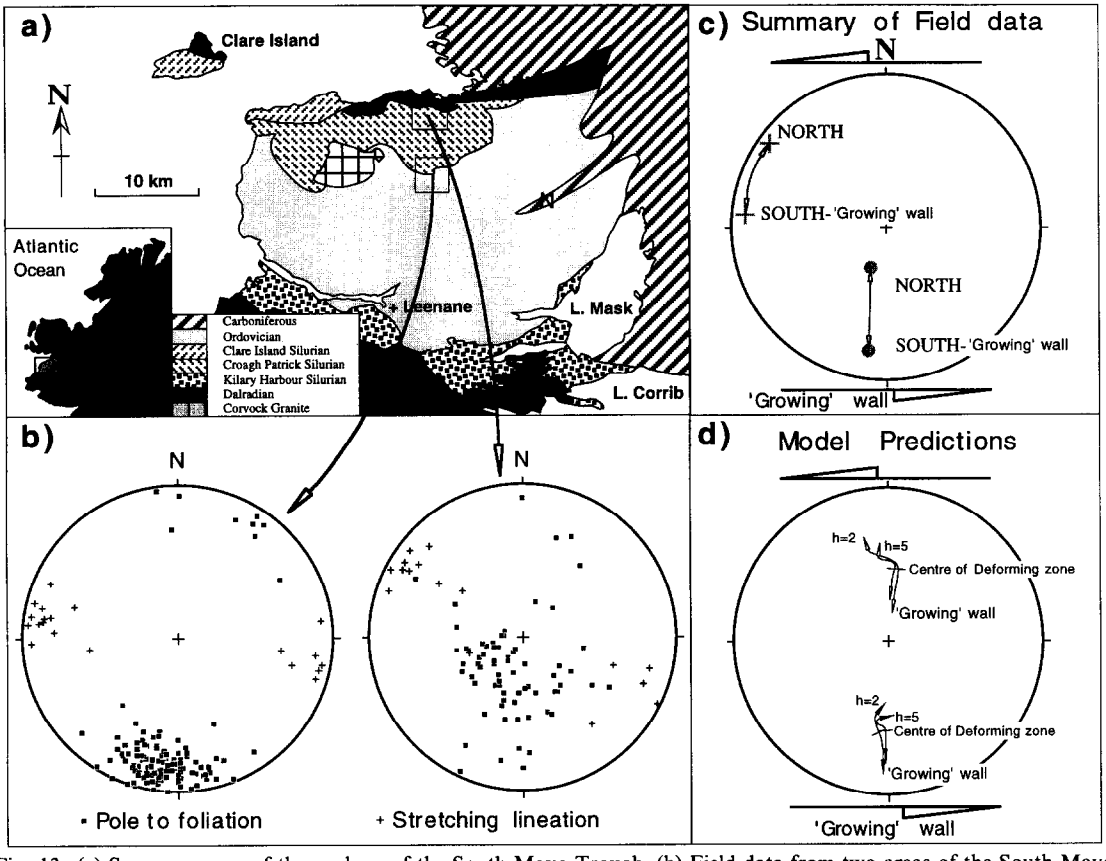

Fig. 13. (a) Summary map of the geology of the South Mayo Trough. (b) Field data from two areas of the South Mayo Trough. (c) Summary of field data. (d) Lower-hemisphere, equal-area stereoplot of foliation (solid arrow heads) and lineation (hollow arrow heads) patterns. Arrows point from the centre of the zone to the edge. The strain applied is equivalent to $\alpha = 50\%$ (the original deforming zone has halved in width), and $\beta = 50°$, $\delta = 45°$. The side of the zone through which new material is incorporated into the deforming zone is indicated as the 'growing' side.

DISCUSSION

The model for transpression with welded boundaries, together with the asymmetric steady-state model for transpression, go some way in explaining the patterns of strain variation across the South Mayo Trough. However, the model does not explain all the variations in strain across South Mayo, nor should it be expected to considering its simplicity.

The models of transpression presented in this paper have many variables. The orientation of the zone boundaries, the height above the 'base' level, the α, β and δ values, as well as whether the deformation zone grew symmetrically or asymmetrically, if at all, must be known. It may be possible to 'tweak' a few or all of these variables to attain a match between the model and a range of field areas. For the South Mayo Trough, the orientation of one zone boundary and the α and δ values are known quite accurately, whereas the other factors are not and can only be estimated. It is difficult to test whether or not the steady-state transpression model is applicable in nature as we only see the end result. One test would be to compare the relative ages of the initiation of deformation. The steady-state transpression model predicts that these should vary systematically across the deforming zone.

The no-slip condition of the boundaries is not always observed in real transpression zones, and many zones do have at least one faulted boundary with dip-slip and/or strike-slip components. Strike-slip faults bounding transpression zones cannot accommodate all the simple-shear strain applied to an area of transpression, and some of this strain must be distributed across the deforming zone if it is to remain a transpression zone. Strain must therefore partition between distributed strain across the zone and strain concentrated in the fault region (Tikoff and Teyssier, 1994; Jones and Tanner, 1995; Teyssier *et al.*, 1995). Dip-slip bounding faults will reduce the concentration of extrusion in the centre of the deforming zone predicted by the Robin and Cruden (1994) transpression model. Strain may partition into dip-slip movements on a bounding fault and distributed strain across the deforming zone, with the extrusion being

concentrated in the centre, as in Sanderson and Marchini (1984) (Fig. 13b).

Acknowledgements—This work was supported by a N.E.R.C studentship. The author wishes to thank John Dewey for setting up the project, general discussion and for reviewing the manuscript. Thanks go also to Neil Selby and Hendrik Jan van Heijst for help with the mathematics.

REFERENCES

Dewey, J. F. (1967) The structural and metamorphic history of the Lower Palaeozoic rocks of central Murrisk, County Mayo, Eire. *Quarterly Journal of the Geological Society of London* **123**, 125–155.

Dewey, J. F. and Ryan, P. D. (1990) The Ordovician evolution of the South Mayo Trough, western Ireland. *Tectonics* **9**, 887–901.

Dias, R. and Ribeiro, A. (1994) Constriction in a transpressive regime: an example in the Iberian branch of the Ibero-Armorican arc. *Journal of Structural Geology* **16**, 1543–1554.

Fossen, H. and Tikoff, B. (1993) The deformation matrix for simultaneous pure shear, simple shear, and volume change, and its application to transpression/transtension tectonics. *Journal of Structural Geology* **15**, 413–422.

Harland, W. B. (1971) Tectonic transpression in Caledonian Spitsbergen. *Geological Magazine* **18**, 27–42.

Hutton, D. H. W. and Dewey, J. F. (1988) Palaeozoic terrane accretion in the western Irish Caledonides. *Tectonics* **5**, 1115–1124.

Jaeger, J. C. (1962) *Elasticity, Fracture and Flow*. John Wiley and Sons, New York.

Jones, R. R. and Tanner, P. W. G. (1995) Strain partitioning in transpression zones. *Journal of Structural Geology* **17**, 793–802.

Kelly, T. J. and Max, M. D. (1979) The geology of the northern part of the Murrisk Trough. *Proceedings of the Royal Irish Academy* **B79**, 191–206.

Lisle, R. J. (1985) *Geological Strain Analysis: A Manual for the R_f/ϕ Technique*. Pergamon, Oxford.

Malvern, L. E. (1969) *Introduction to the Mechanics of a Continuous Medium*. Prentice-Hall, Englewood Cliffs, New Jersey.

McKerrow, W. S. and Campbell, C. J. (1960) The stratigraphy and structure of the Lower Palaeozoic rocks of NW Galway. *Scientific Proceedings of the Royal Dublin Society* **A1**, 27–51.

Ramsay, J. G. (1967) *Folding and Fracturing of Rocks*. McGraw-Hill, New York.

Ramsay, J. G. and Graham, R. H. (1970) Strain variation in shear belts. *Canadian Journal of Earth Sciences* **7**, 786–813.

Robin, P.-Y. F. and Cruden, A. R. (1994) Strain and vorticity patterns in ideally ductile transpression zones. *Journal of Structural Geology* **6**, 447–466.

Ryan, P. D. and Dewey, J. F. (1991) A geological and tectonic cross-section of the Caledonides of western Ireland. *Journal of the Geological Society of London* **148**, 173–180.

Ryan, P. D., Sawal, V. K. and Rowlands, A. S. (1983) Ophiolite melange seperates ortho and paratectonic Caledonides in western Ireland. *Nature* **302**, 50–52.

Sanderson, D. J. and Marchini, W. R. D. (1984) Transpression. *Journal of Structural Geology* **6**, 449–458.

Schwerdtner, W. M. (1989) The solid-body tilt of deformed paleohorizontal planes: an application to an Archean transpression zone, southern Canadian Shield. *Journal of Structural Geology* **11**, 1021–1027.

Teyssier, C., Tikoff, B. and Markley, M. (1995) Oblique plate motion and continental tectonics. *Geology* **23**, 447–450.

Tikoff, B. and Teyssier, C. (1994) Strain modeling of displacement-field partitioning in transpressional orogens. *Journal of Structural Geology* **16**, 1575–1588.